ELECTRON-LATTICE INTERACTION:

AZULENE IN NAPHTHALENE

by

Peter CERVENKA

SUBMITTED IN PARTIAL FULFILMENT OF THE REQUIREMENTS FOR THE DEGREE

OF MASTER OF SCIENCE IN THE PHYSICS DEPARTMENT

OF THE SCHOOL OF ARTS AND SCIENCES,

AMERICAN UNIVERSITY OF BEIRUT

BEIRUT, LEBANON

BEIRUT

1966

ELECTRON-LATTICE INTERACTION:

AZULENE IN NAPHTHALENE

CERVENKA

ACKNOWLEDGMENTS

The author wishes to express his deep gratitude to his advisor Dr. Antoine B. Zahlan for his help and careful guidance throughout all of this work.

Acknowledgments are also due to the technical staff of the Physics Department at the American University of Beirut who built much of the experimental apparatus for the research.

The help of Professors H.J. Maria and J.W. McClain who read the manuscript and gave valuable suggestions is gratefully acknowledged.

To Mr. Pierre Jamous we extend our thanks for his excellent typing.

Last but not least, many thanks go to the author's parents for their continued moral and financial support.

A B S T R A C T

The investigation of the $^1A_1 \rightarrow {}^1B_1$ transition of azulene in crystalline naphthalene is reported. Our study reveals that the oscillator strength of the 0-0 transition at 14,652 cm^{-1} is constant between 4.2°K and 55°K. The 0-0 + 664 vibronic line is affected by a 54 cm^{-1} lattice phonon. The 0-0 + 857 and 0-0 + 2 x 857 bands show a decrease in oscillator strength due to a 46 cm^{-1} phonon. A 15 cm^{-1} lattice phonon reduces the oscillator strength of the 0-0 + 384 + 1386, 16,510 - 16,540 and 0-0 + 1191 + 1386 plus 0-0 + 2 x 664 + 1386 vibronic bands. The band half-widths do not exhibit any significant change between 4.2°K and 100°K.

TABLE OF CONTENTS

LIST OF TABLES

LIST OF FIGURES

Figure Page

I. INTRODUCTION

Bicyclo-[0.3.5] -deca-1.3.5.7.9-pentaene or azulene has a structural formula shown in Figure 1. New compounds derived from azulene are usually numbered according to scheme (I) whereas those derived from bicyclo-[0.3.5]-decane follow scheme (II).[1]

A review of the most significant work done on this compound should mention a 1955 paper by Beer and Longuet-Higgins[2] reporting three different anomalous effects. These results were to be soon afterwards confirmed by Viswanath and Kasha.[3] These workers reported that in azulene, fluorescence emission occurs from the second excited singlet state. That is, no normal fluorescence has been observed from the first excited singlet state, as is usually the case in this class of hydrocarbons. Finally, no triplet-singlet phosphorescence whatsoever has been detected.

The absorption spectrum of azulene vapour was known at the time these data were published, as it had been studied between 21°C and 74°C in the visible and between 127°C and 291°C in the ultraviolet region and reported in 1947 by Heilbronner and Wieland.[4] New interest in this compound resulted in the publication of the results of these new experiments. Polarized light was used in the study of single crystals, as radiation from different lines in the spectrum is polarized along certain distinct directions. This procedure was used by Hunt and Ross in the infra-red region, principally between 300 cm^{-1} and 2000 cm^{-1}. Their work in the infra-red also includes the study of azulene in the vapour and in solution.[5] Besides that, Hunt and Ross have measured the absorption spectrum of a pure azulene crystal at 4°K.[6] The

Fig. 1.--Structural formulae of azulene

Fig. 1

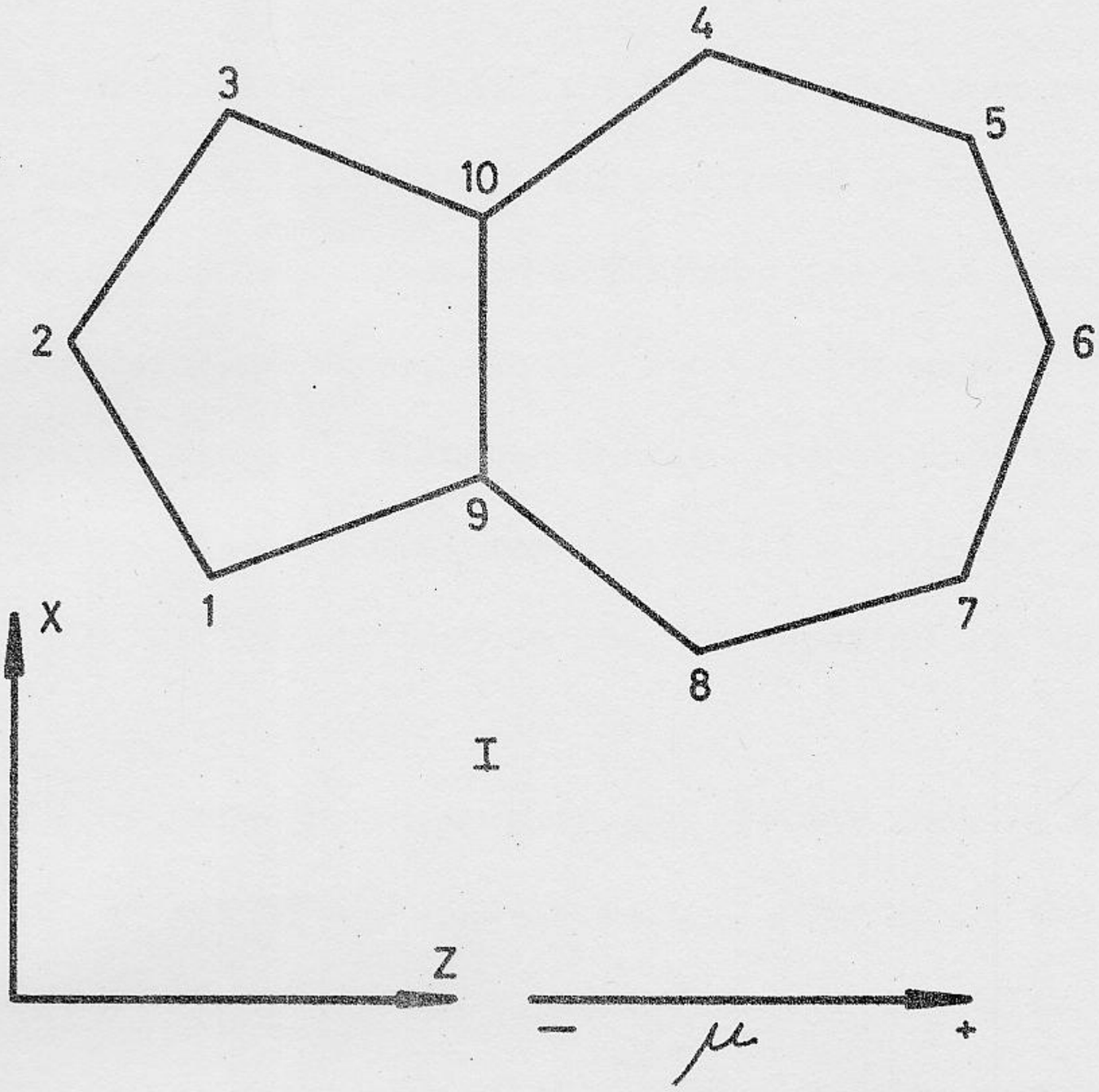

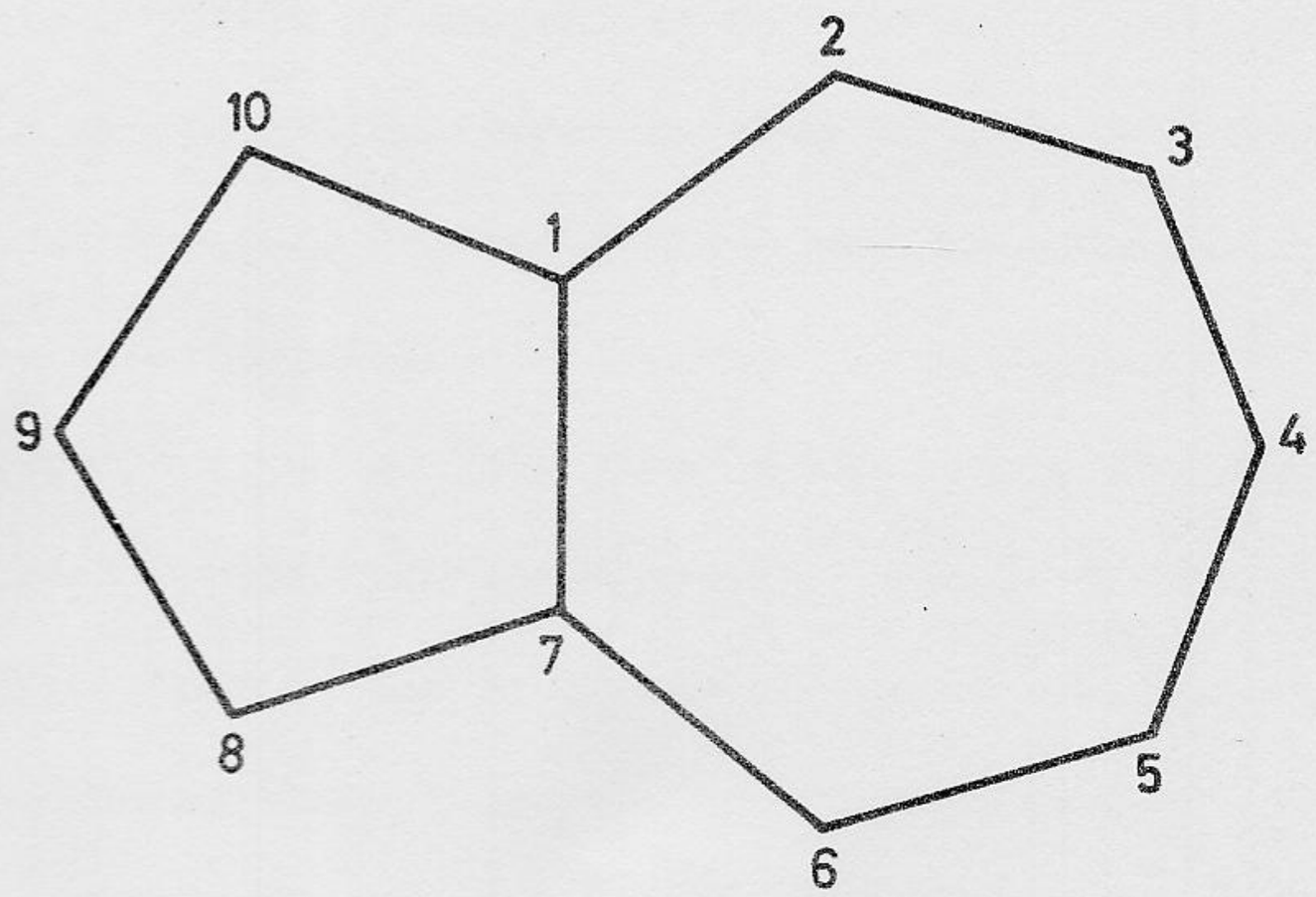

II

absorption of crystalline azulene at 1.5°K has also been reported.[7]

In a pure crystal, excitons are scattered by the phonons and this leads to line broadening. Phonons may reduce the site symmetry and favour some otherwise forbidden transitions. Such is the case in benzene[8] and crystalline naphthalene.[9] Although one can deduce from the investigation of mixed crystals that the electronic excitation in guest molecules is affected by the lattice phonons, no one has reported any detailed study of this effect.

It is precisely the purpose of the present work to give experimental results on the effect of naphthalene lattice phonons on the electronic transitions $^1A_1 \rightarrow {}^1B_1$ of the guest molecule, azulene. The 0-0 transition at 14,652 cm^{-1} has a moment polarized along the molecular x-axis. The oscillator strengths and line widths of certain representative parts of the spectrum of single crystals of azulene in naphthalene are examined as the sample is taken from liquid helium temperature up to room temperature. Information is gained about the coupling between the azulene molecule and the naphthalene lattice. The naphthalene absorption edge is at 32,000 cm^{-1}. The emission and absorption spectrum has been reported by Sidman and McClure. The azulene enters the mixed crystal substitutionally[10] and in such small quantities (less than 0.1%) that it can be considered as an impurity. The presence of greater concentrations of azulene in the mixture may create a micro-crystalline pure azulene phase.

The polarized red absorption system of azulene in naphthalene[10] in the bc' plane has a high extinction coefficient along the b axis while it

vanishes along the c' axis. It was thus possible to conduct without any drawback our research using nonpolarized light.

II. THEORY

The spectrum of azulene has interested many workers.[11-23] We shall in what follows show some of the salient characteristics of this molecule that are deducible from group theoretical considerations. For a qualitative treatment of the physical quantities that can be otherwise obtained from experimental data, we shall give an account of the work of Pariser.

Considering that azulene has structural formula (I) shown in Figure 1 and taking our z-axis to be the long axis of the molecule, the pi-electronic states of the azulene molecule can be seen to belong to the symmetry group C_{2v} irreducible representations. The pi-electrons are associated with 8-shaped clouds in which each branch has a different sign, the molecular plane is not a plane of symmetry of the wave function. The A_2 and B_2 irreducible representations of symmetry group C_{2v} are therefore not admissible.

TABLE 1

IRREDUCIBLE REPRESENTATIONS OF SYMMETRY GROUP C_{2v}

	C_{2v}	E	C_2	$\sigma_{v(zx)}$	$\sigma_{v(yz)}$
(z)	A_1	1	1	1	1
	A_2	1	1	-1	-1
(x)	B_1	1	-1	1	-1
(y)	B_2	1	-1	-1	1

We now examine the value of the matrix elements whose square gives the transition probabilities and consider $\langle \psi_f | \vec{r} | \psi_i \rangle$ where ψ_i is the wave function describing the initial state, ψ_f is the wave function describing the final state and

$$\vec{r} = x\,\hat{i} + y\,\hat{j} + z\,\hat{k} \qquad (1)$$

If we take $\vec{r} = x\,\hat{i}$ and notice that x in the character table belongs to the B_1 irreducible representation, then the direct product for example of

$$A_1 B_1 \Gamma(x) = A_1 B_1 B_1 = A_1 \qquad (2)$$

the totally symmetric representation. Therefore the short axis polarized electronic transition $A_1 \rightarrow B_1$ is symmetry allowed in azulene (or any other C_{2v} molecule). The long axis polarized transition is given by

$$A_1 B_1 \Gamma(z) = A_1 B_1 A_1 = B_1 \qquad (3)$$

We can conclude from all this that $A_1 \rightarrow B_1$ transitions are short axis polarized and that all z-axis polarized transitions $A_1 \rightarrow B_1$ are forbidden.

We now focus our attention on the treatment given by Pariser.[24] The Pariser-Parr method is applied to compute the pi-electron energies, transition moments, charge distributions and bond orders of the ground state and the lower singlet and triplet states. Two parallel calculations are carried through, one starting with conventional Huckel molecular orbitals and the other with perimeter molecular orbitals.

For the pi-electron dipole moment of the ground state, Pariser calculates a value of 1.88 D with Huckel molecular orbitals and 3.66 D with perimeter molecular orbitals. The experimental value is 1.0 D.[14] In this connection, it is interesting to notice that the dipole moments of most of the excited states are opposite or at right angles to the ground state dipole moment.

Fig. 2.--Energy levels of azulene according to Mann et al and following Pariser's notation.

Fig. 2

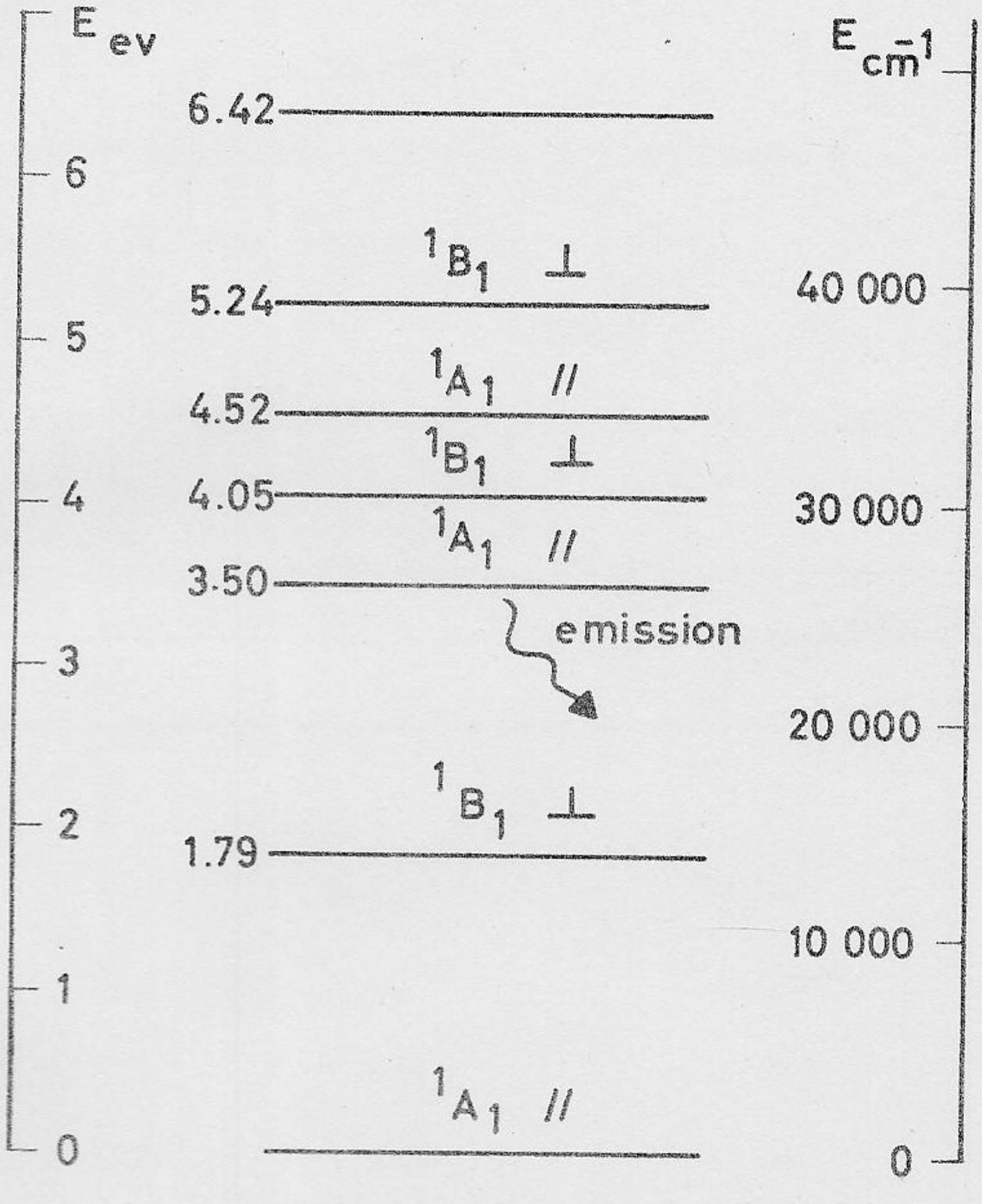
E ev
E cm⁻¹
6.42
6
$^1B_1$ ⊥
5.24
40 000
5
$^1A_1$ //
4.52
$^1B_1$ ⊥
4
4.05
30 000
$^1A_1$ //
3.50
emission
3
20 000
$^1B_1$ ⊥
2
1.79
10 000
1
$^1A_1$ //
0
0

The energies and oscillator strengths calculated by Pariser are compared with the experimental values based on Mann et al,[11] Table 2. In this table, $^1A_1$ || means that the transition considered is between the ground state $^1A_1$, and another $^1A_1$ state and is directed parallel to the long, or z-axis. $^1B_1$ ⊥ on the other hand, means that we are considering a transition between the same ground state and an excited state $^1B_1$, along the short axis, x, or perpendicularly to the long axis.

The theoretical calculations using Huckel molecular orbitals are in good agreement with the experimental values.

TABLE 2

COMPARISON WITH EXPERIMENT OF HUCKEL MO ENERGY CALCULATION WITH INTERACTION OF ALL SINGLY EXCITED CONFIGURATIONS

State	Calculated		Experimental	
	E(ev)	f	E(ev)	f
$^1A_1$	0	0	0	0
$^1B_1$ ⊥	1.732	0.017	1.79	0.009
$^1A_1$ ||	3.084	0.002	3.50	0.08
$^1B_1$ ⊥	4.112	0.116	4.05?	?
$^1A_1$ ||	4.692	1.243	4.52	1.10
$^1B_1$ ⊥	5.604	0.365	5.24	0.38
$^1A_1$ ||	5.994	0.003	6.42	0.65
$^1B_1$ ⊥	6.191	0.014		
$^1A_1$ ||	6.867	0.215		
$^1B_1$ ⊥	7.018	0.278		
$^1A_1$ ||	7.018	0.199		

III. EXPERIMENTAL

1. Material Used

The naphthalene used was of zone refined purity. The azulene was a chromatographed sample provided by Dr. George H. Heilmeir of R.C.A. Laboratories, Princeton, N.J.

Several crystals of different azulene concentrations and thickness in the range 1 - 10 mm had to be used to cover the temperature range 4.2°K to 300°K and to investigate lines of different intensities. The azulene concentration in the crystals used was found by dissolving the sample in absolute ethanol and comparing the optical density with that of a known concentration of azulene in absolute ethanol solution. In doing this, the visible part of the azulene spectrum was used. In this optical region the naphthalene does not contribute to the absorption.

This operation was kindly run for us on a Unicam Spectrophotometer-Comparator in the Chemistry Department, American University of Beirut, by Dr. George Hanania.

Using this method, the azulene concentration in different crystals was found to be 10^{-3} - 10^{-4} moles per mole of naphthalene. In this azulene concentration range, the half-widths of the 0-0 and vibronic lines at 4.2°K are of the order of 20 cm^{-1}.

2. The Oven

Single crystals of azulene in naphthalene were grown from the melt using the Bridgman method. A vertical oven was constructed according to details given in the literature[25] and the whole crystallization process could be observed. The vessel containing the melt was suspended in the

Fig. 3.--Crystal-growing oven

Fig. 4.--Typical temperature distribution curve inside the oven

Fig. 3

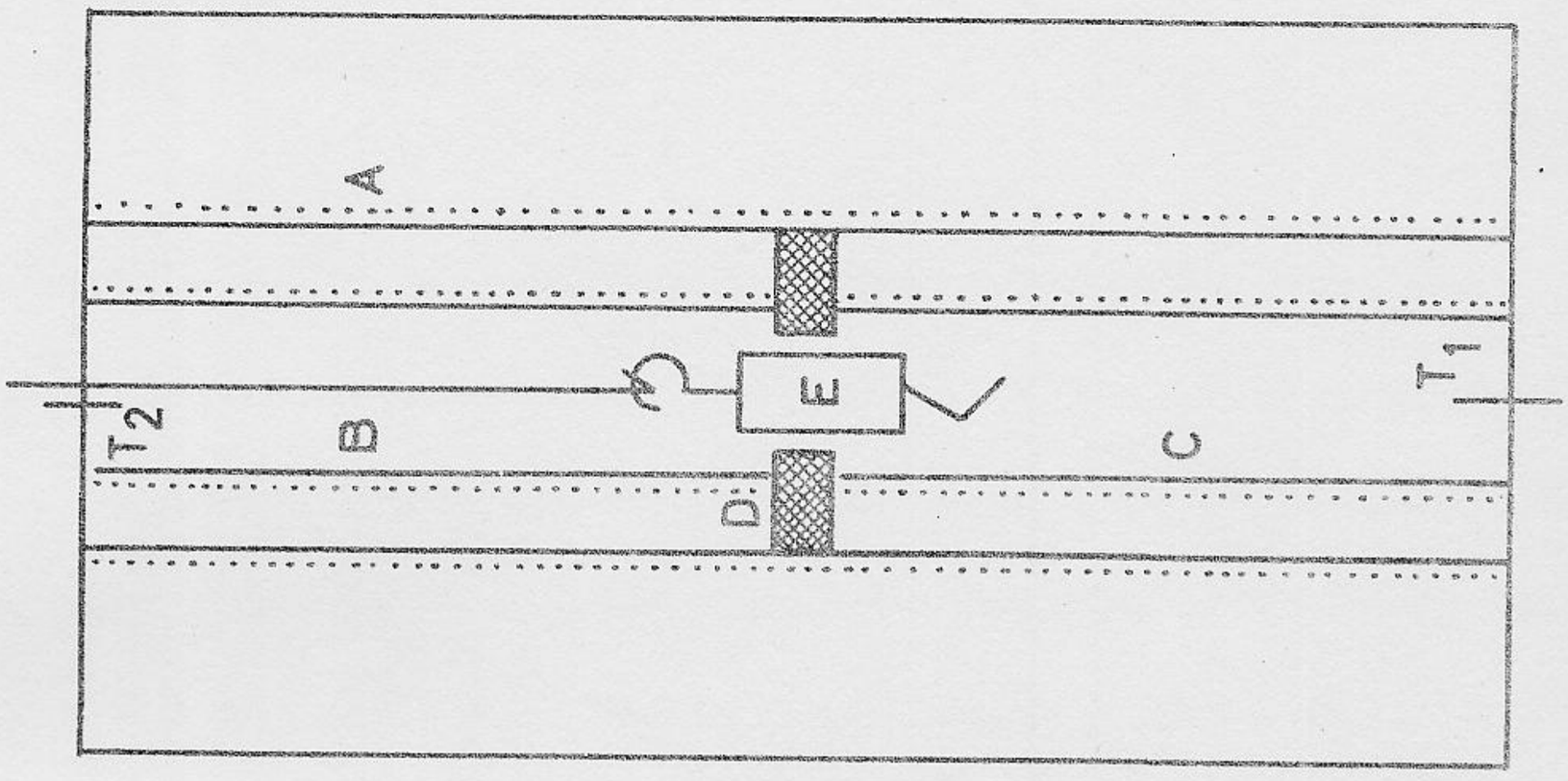

Fig. 4

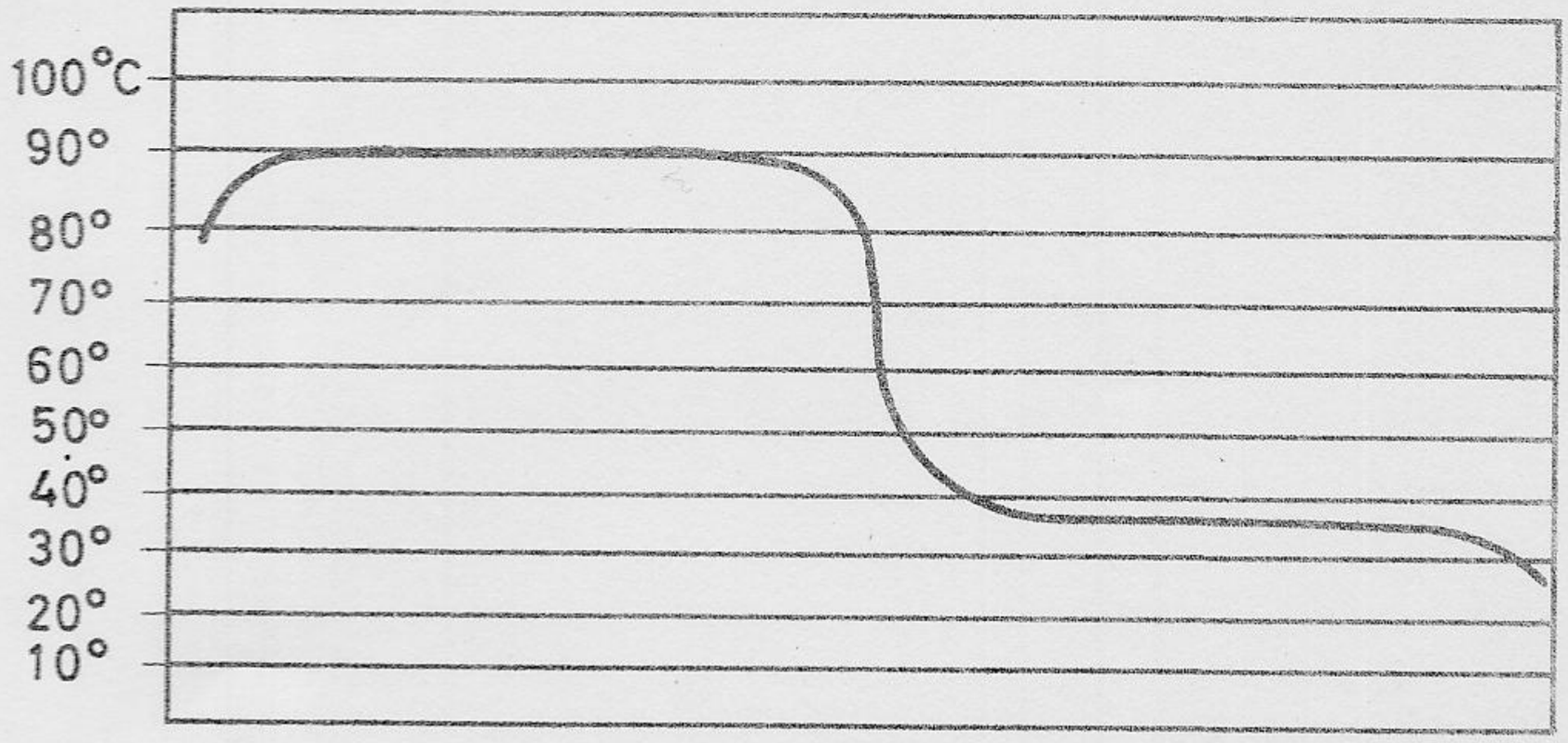

upper part of the furnace, where the temperature was above the melting point of the azulene and naphthalene mixture.

The vessel was lowered very slowly (at a rate of about 1-2 mm per hour) down the temperature gradient. As the tip of the vessel passed the middle of the oven, crystallization began and this process continued as the growth vessel kept on descending.

The oven is made of two concentric Pyrex cylinders. The inner cylinder is cut into two equal parts. The halves of this inner cylinder are separated by a Marinite stopper open in the middle so as to allow the growth tube to pass through. Figure 3 shows the details of the oven with the outer cylinder A and the inner two half-cylinders B and C which are separated by the stopper D into which the growth vessel E is passing. Resistance wire is wound as a spiral around the inner and outer cylinders and two Thermistemp Model 63 RA temperature regulators are included at the top and bottom of the furnace.

In the upper part of the oven a circular hole is cut into the Marinite. The crystal growing vessel E is introduced through this hole. When in use, this hole is closed by means of a lid containing one of the Thermistemp sensors. The crystal growth tube is supported by a fine metal wire passing through a small hole in this lid.

The outer part of the oven is made out of Marinite except the front which is a sliding piece of thick glass so that one can watch the entire crystallization process.

The inner, upper and lower heaters are controlled automatically by the sensors while the current in the outer coil is set to a fixed value.

Fig. 5.--Growth vessel

Fig.5

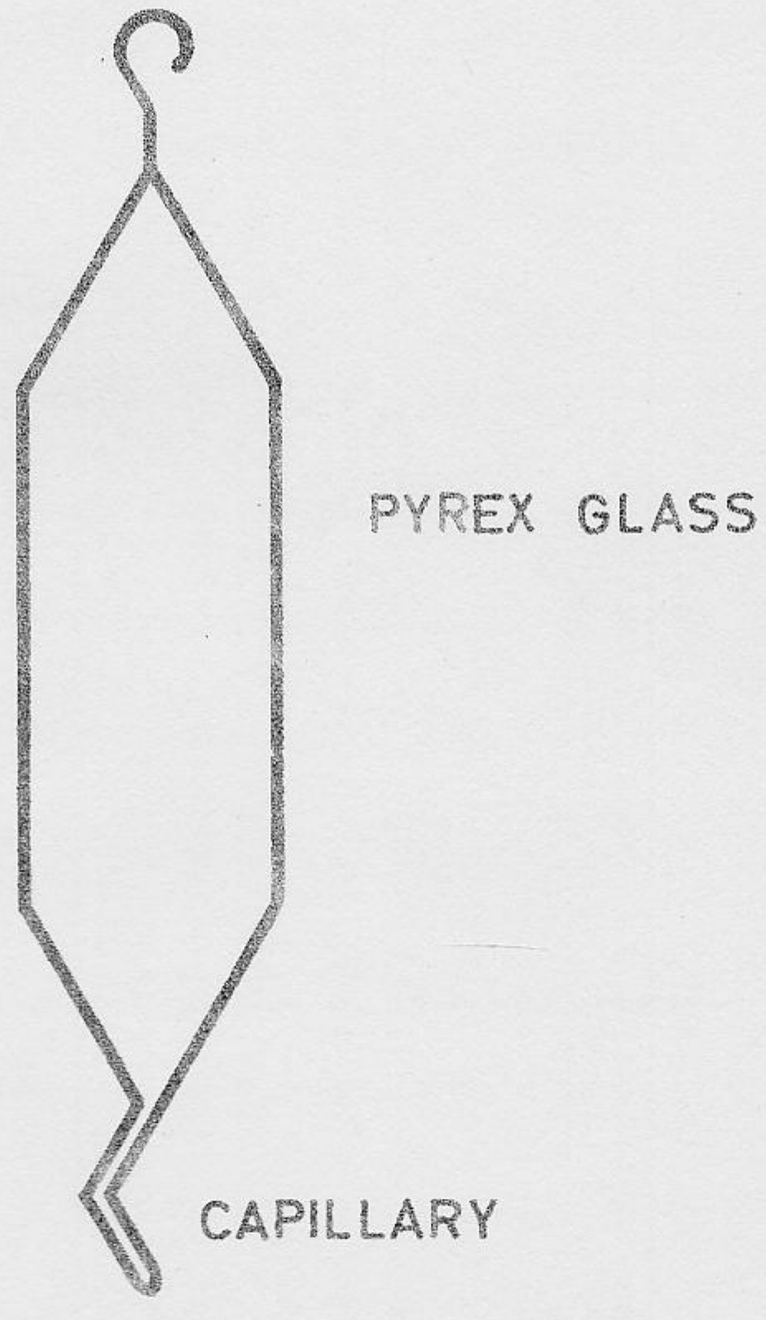

A more refined model of the oven which was built later included two separate outer heaters which gave the instrument more flexibility for the choice of the inner temperatures.

3. The Temperature Gradient

One could change the values of the currents in the three coils so as to get a suitable temperature gradient. The graph of temperature against position is shown for a typical setting in Figure 4. This graph looks like a step function and the more abrupt the change of temperature in the middle of the oven, the better the chances are of getting a good crystal.

4. The Growth Vessel

The type of vessel used is shown in Figure 5. As the Pyrex container, which can be about 15 centimeters in length, is lowered in the oven, the little curved tail which is a capillary tube starts to solidify and produces the crystal seeds which are responsible for the production of large single crystals.

5. The Method of Filling the Growth Vessel

Figure 6 shows schematically the set-up for filling the material to be crystallized. Zone-refined naphthalene was introduced into a Pyrex bowl and a few specks of azulene were put directly into the growth vessel. The system was then connected through a trap to a vacuum pump and when the pressure was sufficiently low (about 10^{-6} mm of mercury) the system was sealed off at point A. Then the naphthalene was distilled by heating the bowl and at the same time cooling the growth vessel part down to liquid nitrogen temperature.

Fig. 6.--Glass system employed to fill growth vessel

Fig. 6

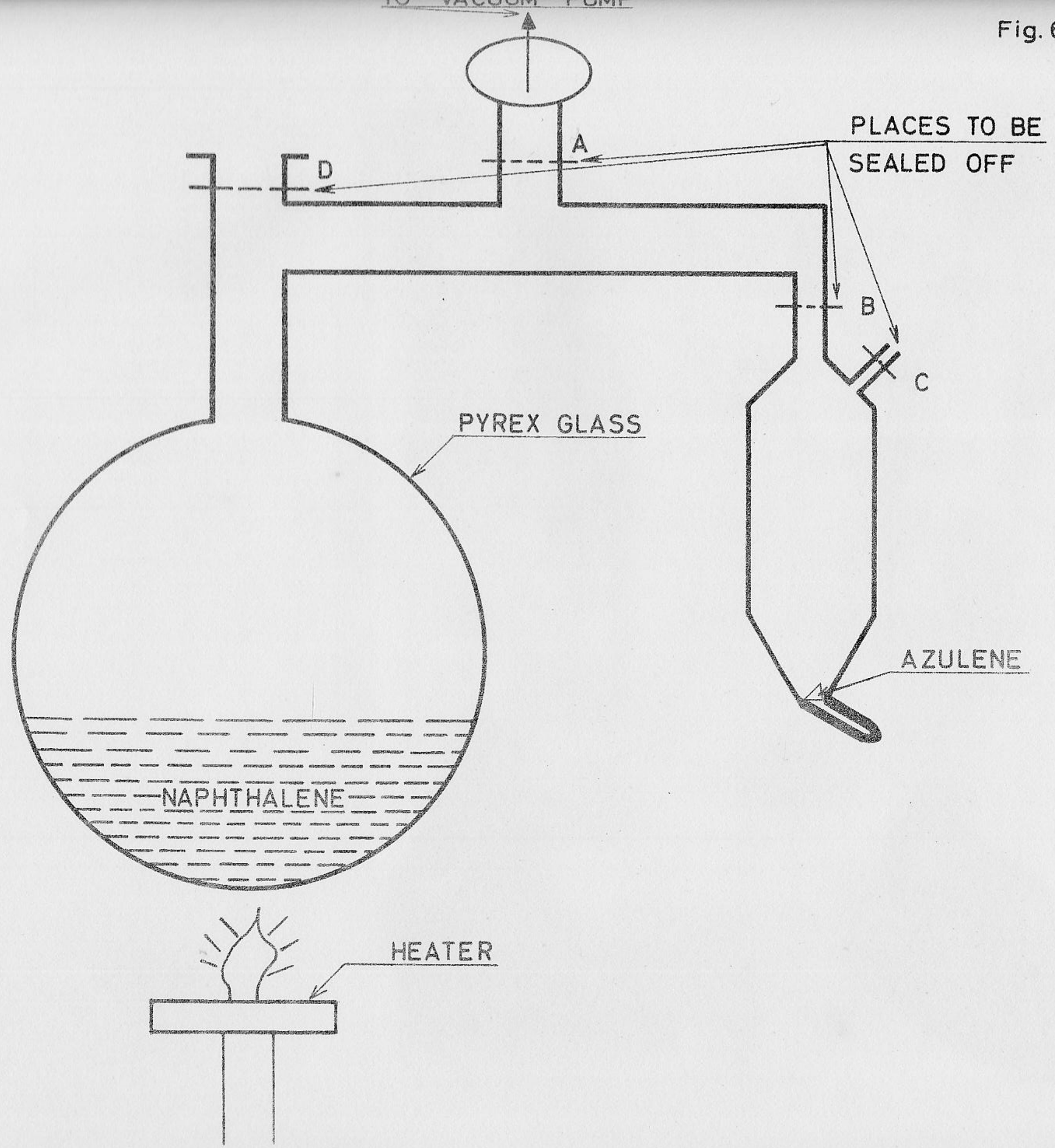
TO VACUUM PUMP
PLACES TO BE SEALED OFF
A
D
B
C
PYREX GLASS
AZULENE
NAPHTHALENE
HEATER

The vessel was sealed off at points B and C (C was used in the first place to get the azulene into the system and D served the same purpose for the naphthalene). Finally, a hook was made on top of the tube which was now separated from the rest and ready for use.

6. The Polishing and Grinding of the Mixed Crystals

The single crystals thus obtained were cut down along their cleavage planes before being used. Thinner crystals were obtained whenever needed by rubbing first on a filter paper soaked in solvent (alcohol, for example), then by polishing against a dry filter paper.

7. A Description of the Spectrograph

The spectrograph used was a Hilger Model E 742. In order to obtain spectra at liquid helium temperature a double Dewar container with quartz windows was used. A Hilger timer Model FS 105 was also used to actuate a shutter. All data were taken with a slit opening of five microns.

8. The Method of Data Analysis and Plate Reduction

The plates (Ilford R40) were run on a Baird Atomic densitometer-comparator and a Bristol Model M-1RB 560-33-T4-T24 chart recorder. Graphs relating the optical density of background intensity to the exposure time (in seconds) were drawn for different wavelengths and only the linear region was used.

Since one has the relationship

$$I = I_o \exp(-kcd) \qquad (4)$$

where I is the measured intensity, I_o the original intensity of the light, k the extinction coefficient, c the concentration and d the thickness of

Fig. 7.--Experimental apparatus

1. Liquid helium Dewar
2. Transfer tube
3. Hoist
4. Liquid air container
5. Vacuum line
6. Light source
7 and 8. Lenses
9. Double Dewar containing the sample
10. Iron arc
11. Temperature measuring apparatus
12. Spectroscope
13. Helium recovery line

the crystal, then it is also true that

$$\log \frac{I}{I_o} = -kcd \qquad (5)$$

The apparatus recorded the logarithm of the ratio of I and I_o and since we were looking for the extinction coefficient we had only to find the area as shown on Figure 8 between the background and the graph coming out of the recorder. This was done with the help of a Haff Model 317 planimeter. The half-widths of the absorption lines under consideration were measured directly from the charts.

9. The Iron Arc and the Position of the Lines

The absorption spectra were calibrated against iron arc lines. The plate was exposed to the arc for about one second. The current in the arc measured around 4 amperes. Once the plates were developed, they were compared with the iron spectrogram taken on a Hilger El quartz spectrograph available from the same company. The linear approximation for the dispersion was used when the lines in the spectrum were to be found very near to our absorption bands. The results, unless otherwise stated, agreed to within 20 cm^{-1} with the values given by Sidman and McClure.

10. The Measurement of Temperature

Various devices were used in different temperature regions. These include:

1) Between room temperature and about 50°K an Engelhard glass enclosed platinum spiral was used. The resistance was measured using a Leeds and Northrup 4735 Wheatstone bridge and a 2430-E galvanometer from the same company.

Fig. 8.--Measurement of half-width and area for a typical band

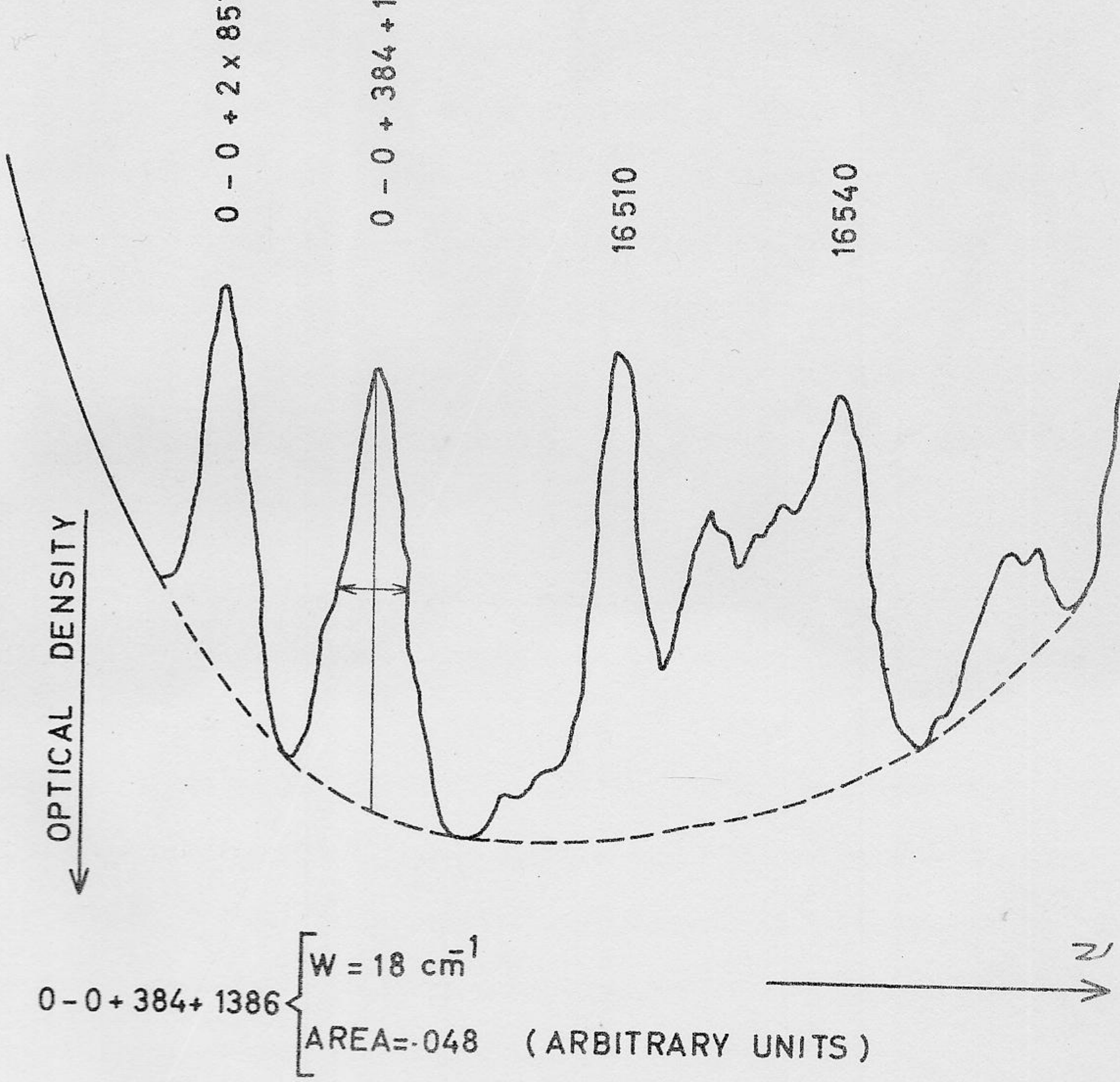
0 - 0 + 2 x 857
0 - 0 + 384 + 1386
16510
16540
OPTICAL DENSITY
0 - 0 + 384 + 1386
W = 18 cm⁻¹
AREA = .048 (ARBITRARY UNITS)
ν

Fig. 8

2) Between 100°K and liquid helium temperature, a Honeywell MHSP 2306 germanium cryogenic thermometer (serial number 1065) was used. The measurement of resistance was done with the help of a Cenco 83412 potentiometer and an Eplab students' cell as a standard.

3) A carbon resistor was also used sometimes and it was calibrated for temperature against the above mentioned germanium resistor. The major drawback when using this type of resistor for temperature measurements is that the resistance at room temperature, liquid nitrogen, and liquid helium temperatures shifts from run to run and even during the same run so that one has to shift the characteristic calibration curve parallel to itself in order to get correct temperature readings. Such a typical calibration curve is represented in Figure 9.

11. Determination of the "best fit" phonon

If the oscillator strength variation is due to optical phonons (this is discussed in more detail later), then the ratio of oscillator strengths should be equal to the ratio of occupation numbers per unit cell. One particular temperature (50°K) was chosen and all the oscillator strengths considered were divided by the oscillator strength at this temperature. On the other hand, the occupation numbers per unit cell for all the optical phonons reported were divided by the corresponding value at 50°K. The results were compared both numerically and graphically and the phonon that gave data within 10 - 15% of our experimental values was chosen.

From the relation giving the value of the oscillator strength as a function of the occupation number per unit cell and coupling constant, the value of α was deduced.

Fig. 9.--Typical calibration curve of a carbon resistance

Fig. 9

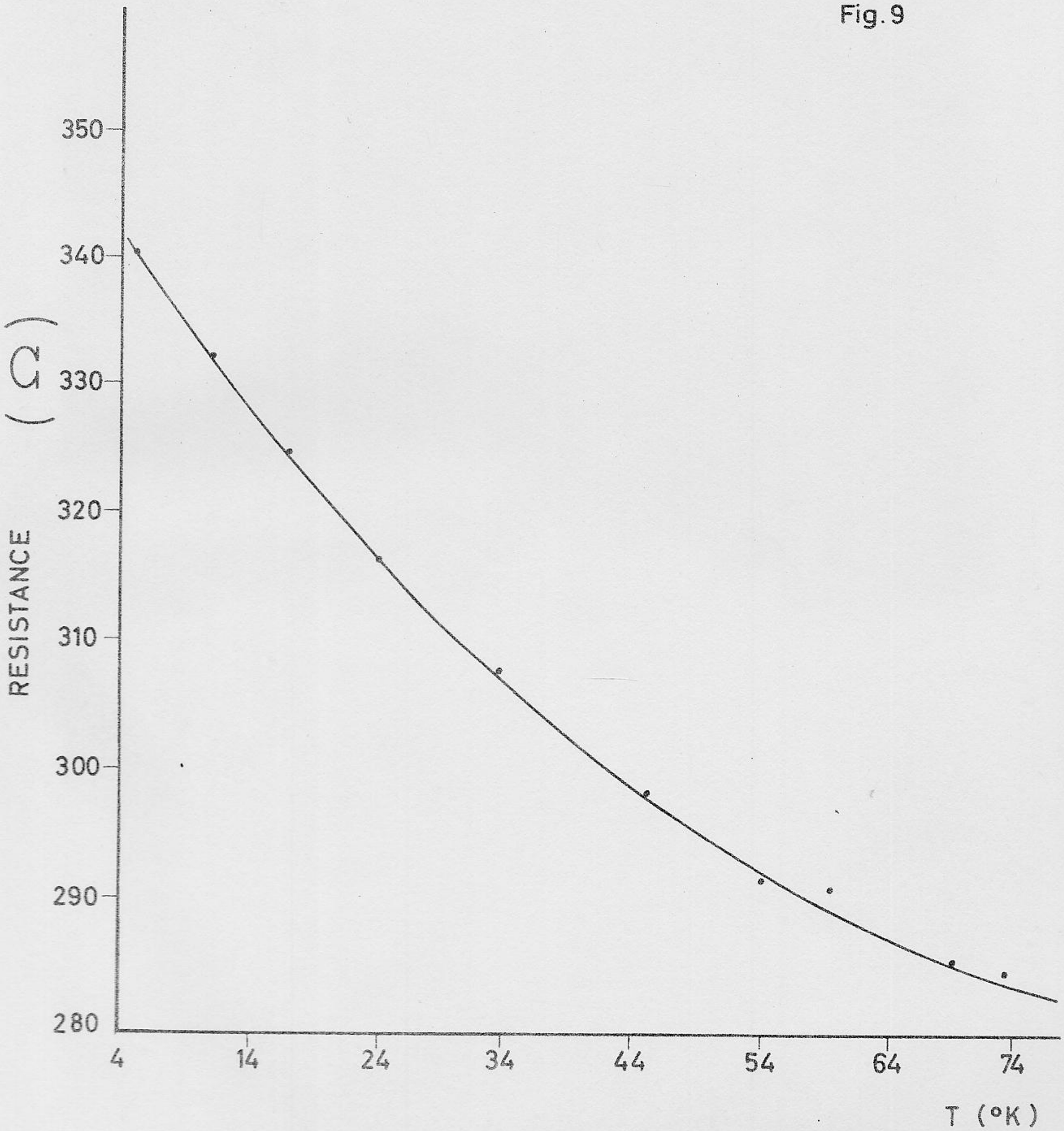
RESISTANCE (Ω)
350
340
330
320
310
300
290
280
4
14
24
34
44
54
64
74
T (°K)

Fig. 10.--Schematic diagram of the spectral region studied

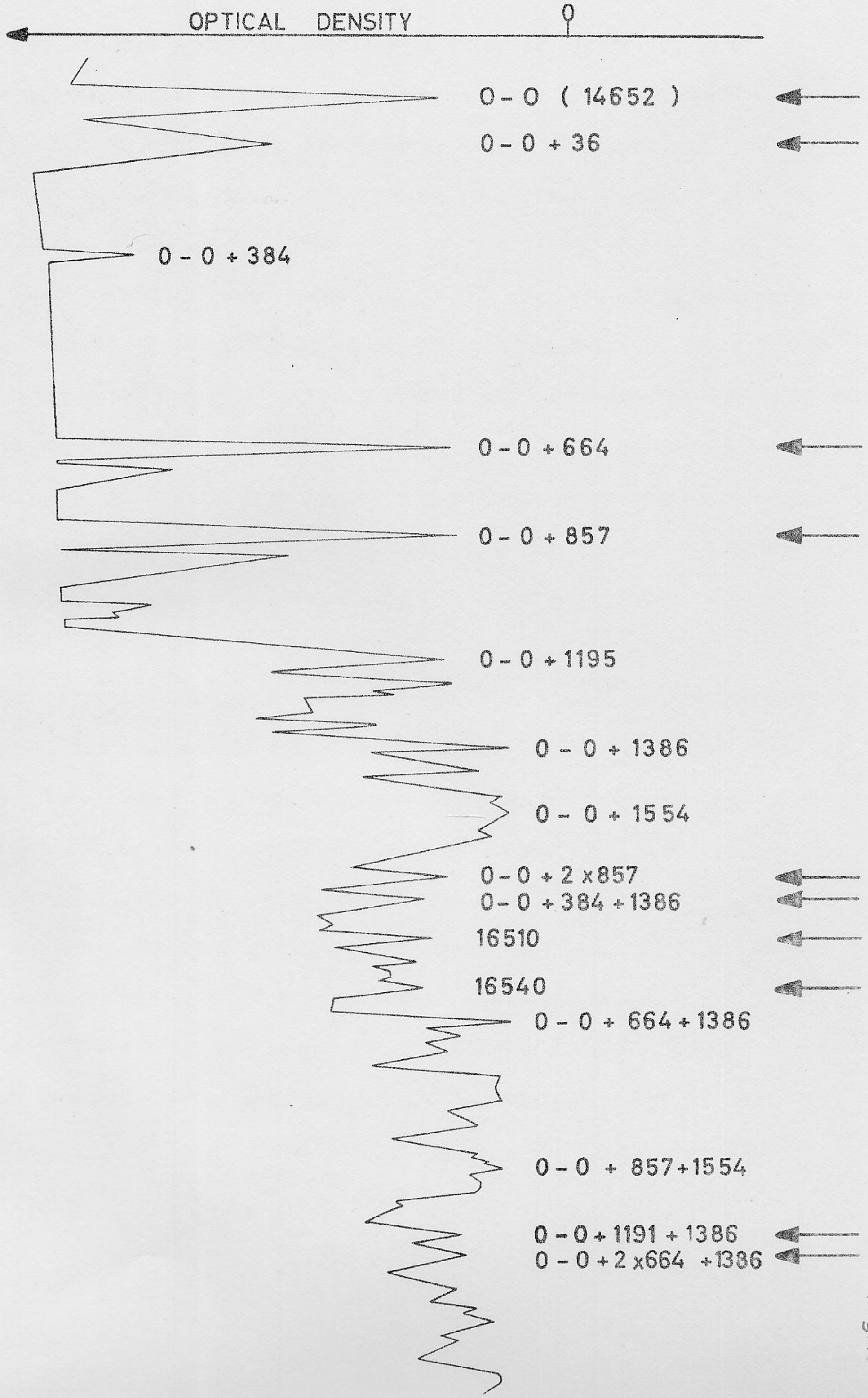
OPTICAL DENSITY
0
0 - 0 (14652)
0 - 0 + 36
0 - 0 + 384
0 - 0 + 664
0 - 0 + 857
0 - 0 + 1195
0 - 0 + 1386
0 - 0 + 1554
0 - 0 + 2 x 857
0 - 0 + 384 + 1386
16510
16540
0 - 0 + 664 + 1386
0 - 0 + 857 + 1554
0 - 0 + 1191 + 1386
0 - 0 + 2 x 664 + 1386
Z

Fig. 10

IV. RESULTS

The spectral region of interest is shown in Figure 10, in which the lines indicated with arrows have been studied. The assignments for the lines are those of Sidman and McClure, except at 16,510 cm^{-1} and 16, 540 cm^{-1} where our values did not come into close agreement with the listed values.

The pure 0-0 electronic lines at 14,652 cm^{-1} could not be separated from the vibronic bands 0-0 + 36 at 14,688 cm^{-1} and 0-0 + 51 at 14,703 cm^{-1} except between 4.4°K and 53°K. The ratio of the oscillator strengths of the 0-0 band and the 0-0 + 36 plus the 0-0 + 51 bands has been computed and is given in Table 3, for the temperature region in which we have data on the individual bands. The ratio of oscillator strengths can be seen to be equal to unity, while the half-width does not vary significantly in the same range.

In order to be able to study the variation over a much wider temperature range, the area of the 0-0, 0-0 + 36 and 0-0 + 51 bands were added up together; this result is shown in Figure 11. Two different crystals were used for the study of the oscillator strength between 4.2°K and 300°K. The variation of $w_{1/2}$ can be seen in Figure 19.

The 0-0 + 664 band at 15,316 cm^{-1} cannot be separated from its vibronic counterparts 0-0 + 664 + 36 and 0-0 + 664 + 51 above 83°K. Between 4.2°K and 83°K where it can be measured, the ratio of the oscillator strengths of the no phonon vibronic and the phonons plus vibronic bands is seen from Table 3 to be equal to 4. The oscillator strength for the sum of the three bands is shown in Figure 12. Here also two different crystals had to be used

Fig. 11.--Oscillator strength (in arbitrary units) of the (0-0) + (0-0 + 36) + (0-0 + 51) bands plotted versus temperature. Two different crystals were used.

Fig. 12.--Oscillator strength (in arbitrary units) of the (0-0 + 664) + (0-0 + 664 + 36) + (0-0 + 664 + 51) bands plotted versus temperature. Two different crystals were used.

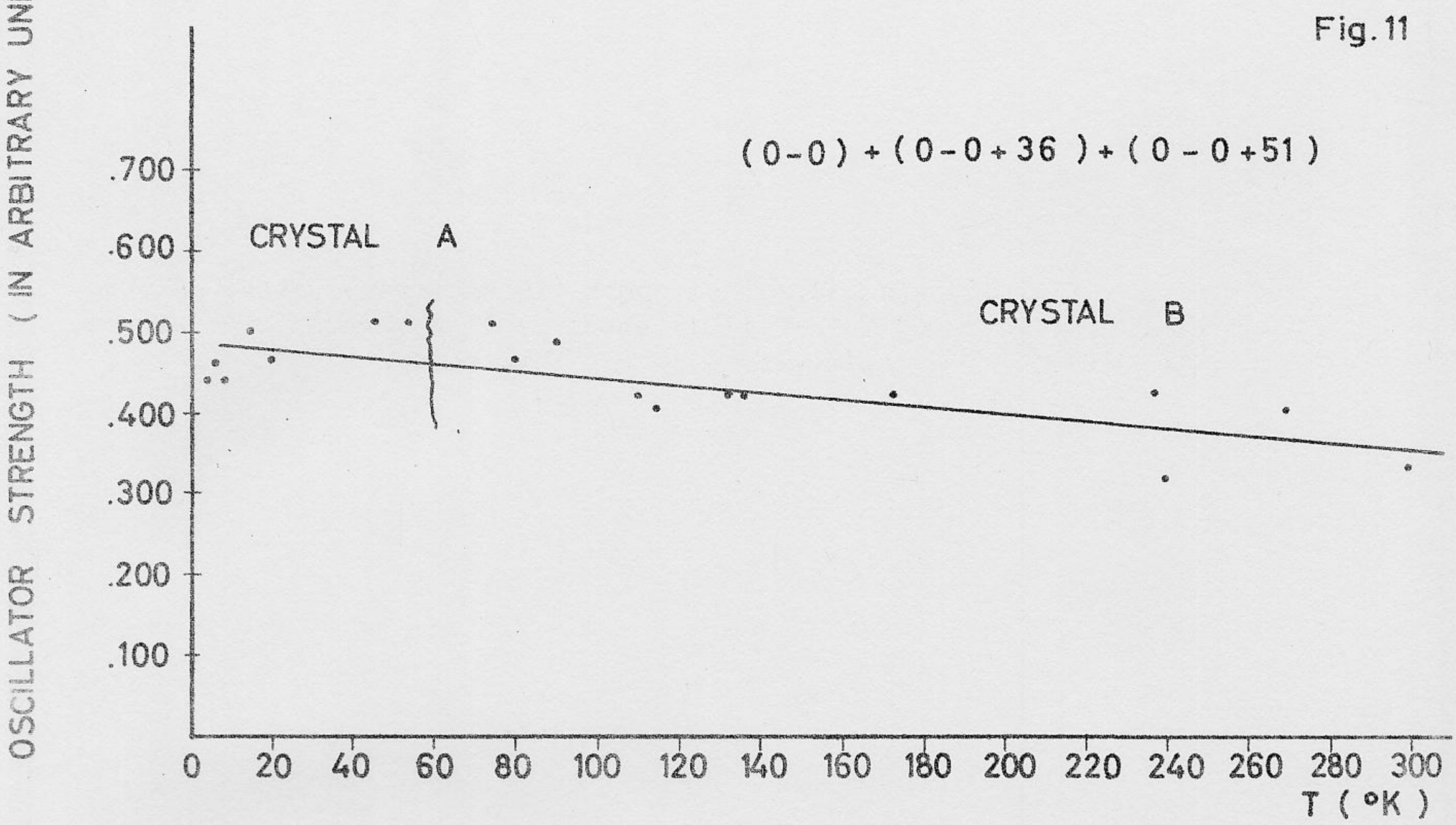

(0-0) + (0-0+36) + (0-0+51)

Fig. 11

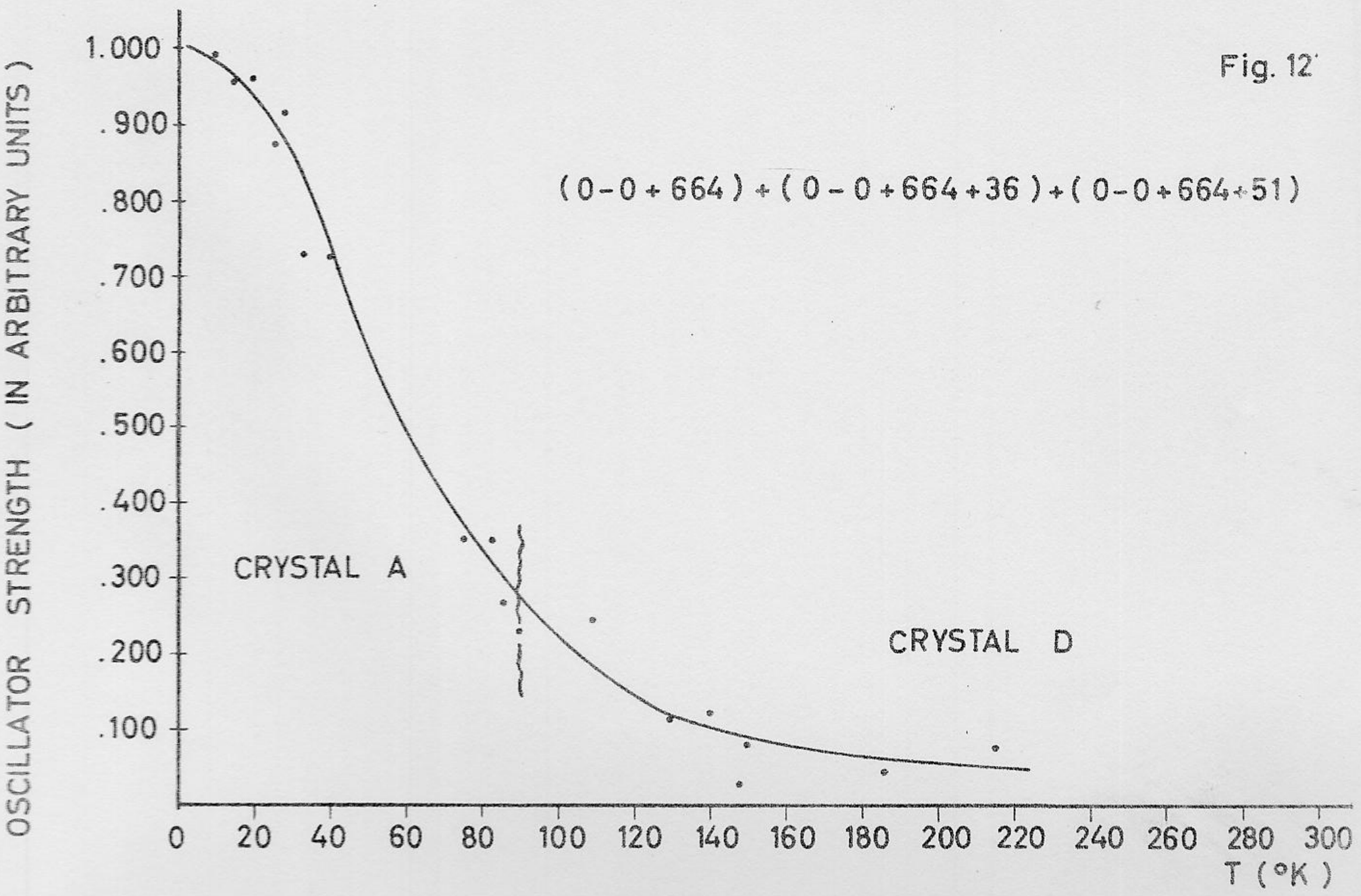

(0-0+664) + (0-0+664+36) + (0-0+664+51)

Fig. 12

Fig. 13.--Half-width of the (0-0 + 664) + (0-0 + 664 + 36) + (0-0 + 664 + 51) bands grouped together plotted versus temperature.

Fig. 13

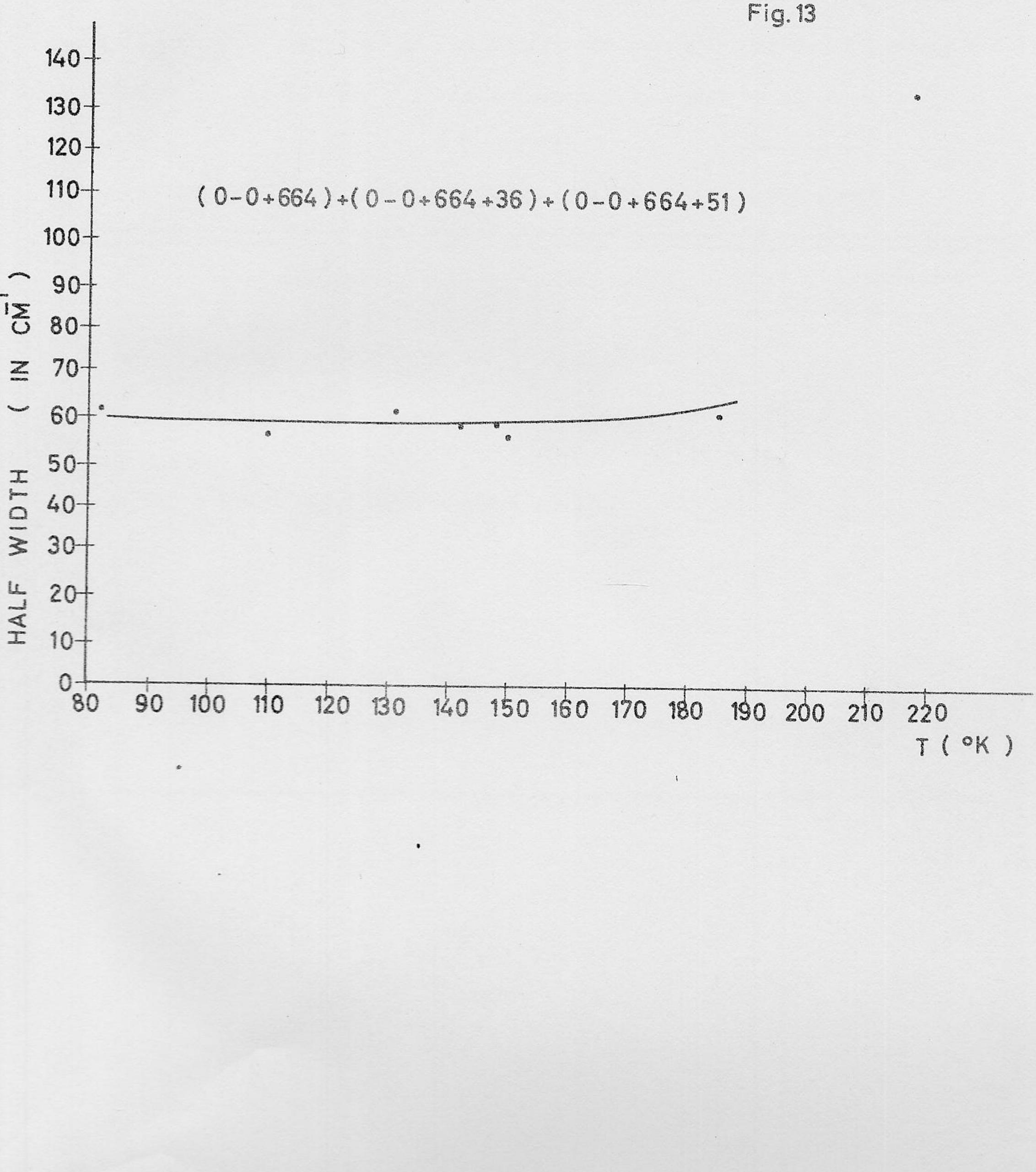
(0-0+664)+(0-0+664+36)+(0-0+664+51)
HALF WIDTH (IN CM^{-1})
140
130
120
110
100
90
80
70
60
50
40
30
20
10
0
80
90
100
110
120
130
140
150
160
170
180
190
200
210
220
T (°K)

within the temperature region considered (4.2°K - 220°K). The half-width of the same bands is seen not to vary appreciably up to 190°K (Figure 13).

Table 3 shows also the results for the 0-0 + 857 system of bands and the variation of the integrated oscillator strength of the 0-0 + 857, 0-0 + 857 + 36 and 0-0 + 857 + 51 bands is plotted against the temperature in Figure 14. The ratio of the oscillator strengths of 0-0 + 857 and 0-0 + 857 + 36 plus 0-0 + 857 + 51 is approximately equal to two.

TABLE 3

RELATIVE OSCILLATOR STRENGTHS OF PURE AND VIBRONIC BANDS

Lines	Half-width	Ratio of Oscillator Strengths
(0-0)/[(0-0 + 36) + (0-0 + 51)]	25 cm^{-1}	1 ± .3 (4.2° - 53°K)
(0-0 + 664)/ [(0-0 + 664 + 36) + (0-0 + 664 + 51)]	18 cm^{-1}	4 ± .9 (4.2° - 83°K)
(0-0 + 857)/ [(0-0 + 857 + 36)+(0-0 + 857 + 51)]	19 cm^{-1}	2 ± .4 (4.2° - 83° K)

Fig. 14.--Oscillator Strength (in arbitrary units) of the (0-0 + 857) + (0-0 + 857 + 36) + (0-0 + 857 + 51) bands plotted versus temperature.

Fig. 14

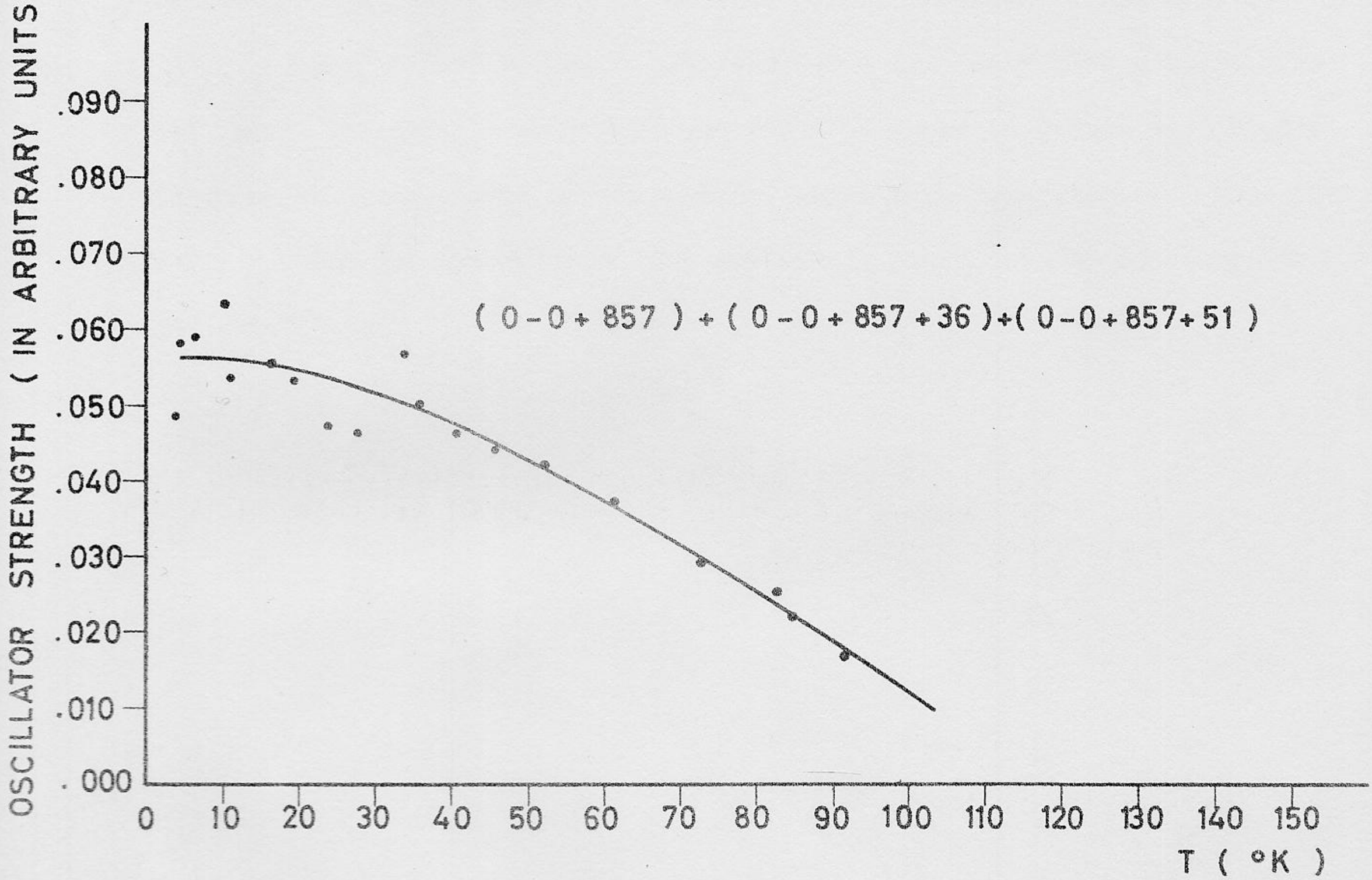
OSCILLATOR STRENGTH (IN ARBITRARY UNITS)
.090
.080
.070
.060
.050
.040
.030
.020
.010
.000
0
10
20
30
40
50
60
70
80
90
100
110
120
130
140
150
T (°K)
(0-0+857) + (0-0+857+36)+(0-0+857+51)

The weaker 0-0 + 2 x 857 and 0-0 + 384 + 1386 bands the oscillator strengths of which are plotted against temperature in Figures 15 and 16 exhibit practically the same character. The area between 16,510 cm^{-1} and 16,540 cm^{-1} has been integrated and the result is shown in Figure 17.

As for the 0-0 + 1191 + 1386 and 0-0 + 2 x 664 + 1386 doublet, its oscillator strength between 4.2° and 160°K is shown in Figure 18. Figure 19 shows the half-widths of the systems which have been studied. Note that 0-0 + 2 x 857 and 0-0 + 384 + 1386 are single lines that do not comprise any satellites.

Fig. 15.--Oscillator strength (in arbitrary units) of the (0-0 + 2 x 857) band plotted versus temperature.

Fig. 16.--Oscillator strength (in arbitrary units) of the (0-0 + 384 + 1386) band plotted versus temperature.

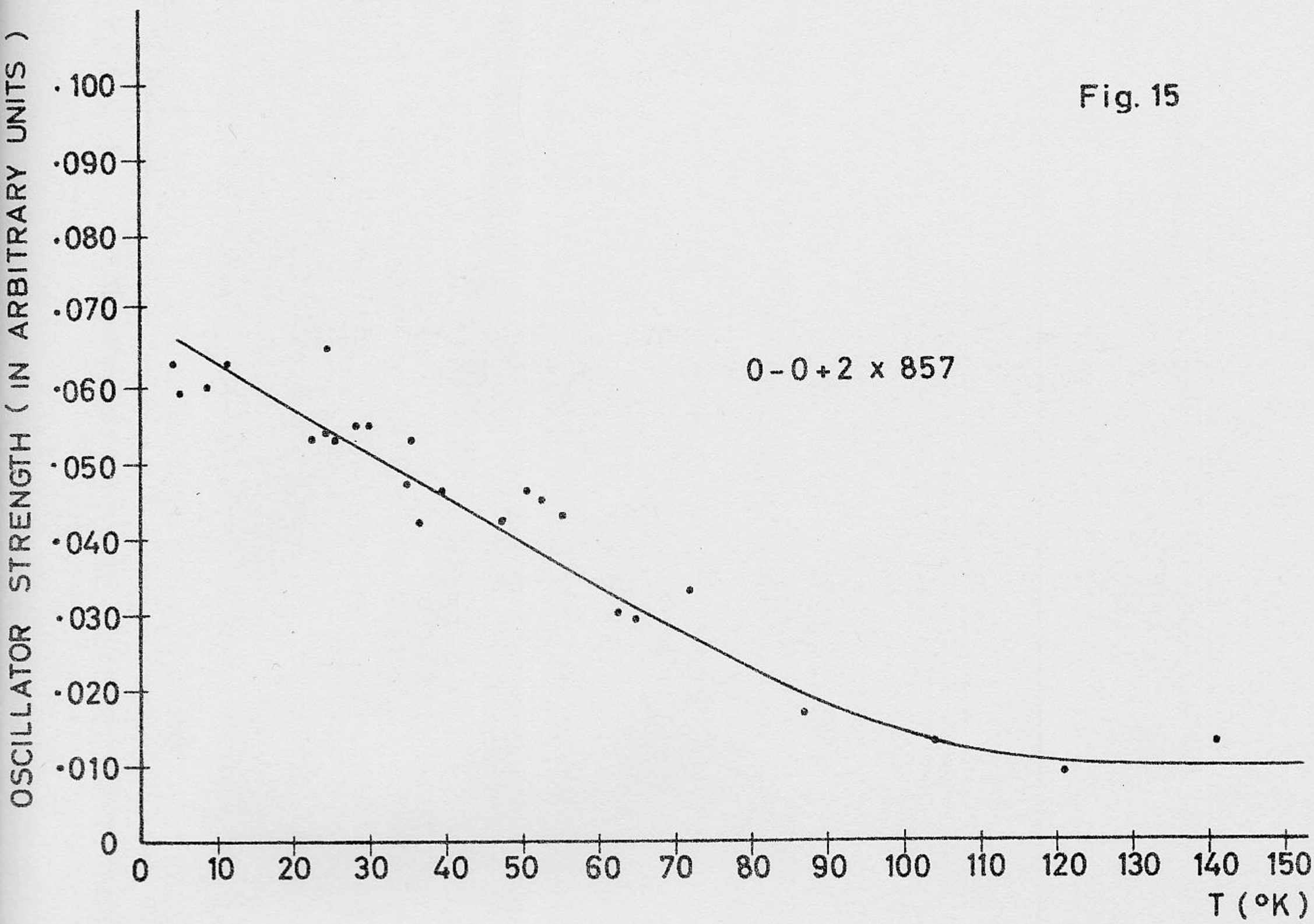
OSCILLATOR STRENGTH (IN ARBITRARY UNITS)
·100
·090
·080
·070
·060
·050
·040
·030
·020
·010
0
0 10 20 30 40 50 60 70 80 90 100 110 120 130 140 150
T (°K)
0-0+2 x 857

Fig. 15

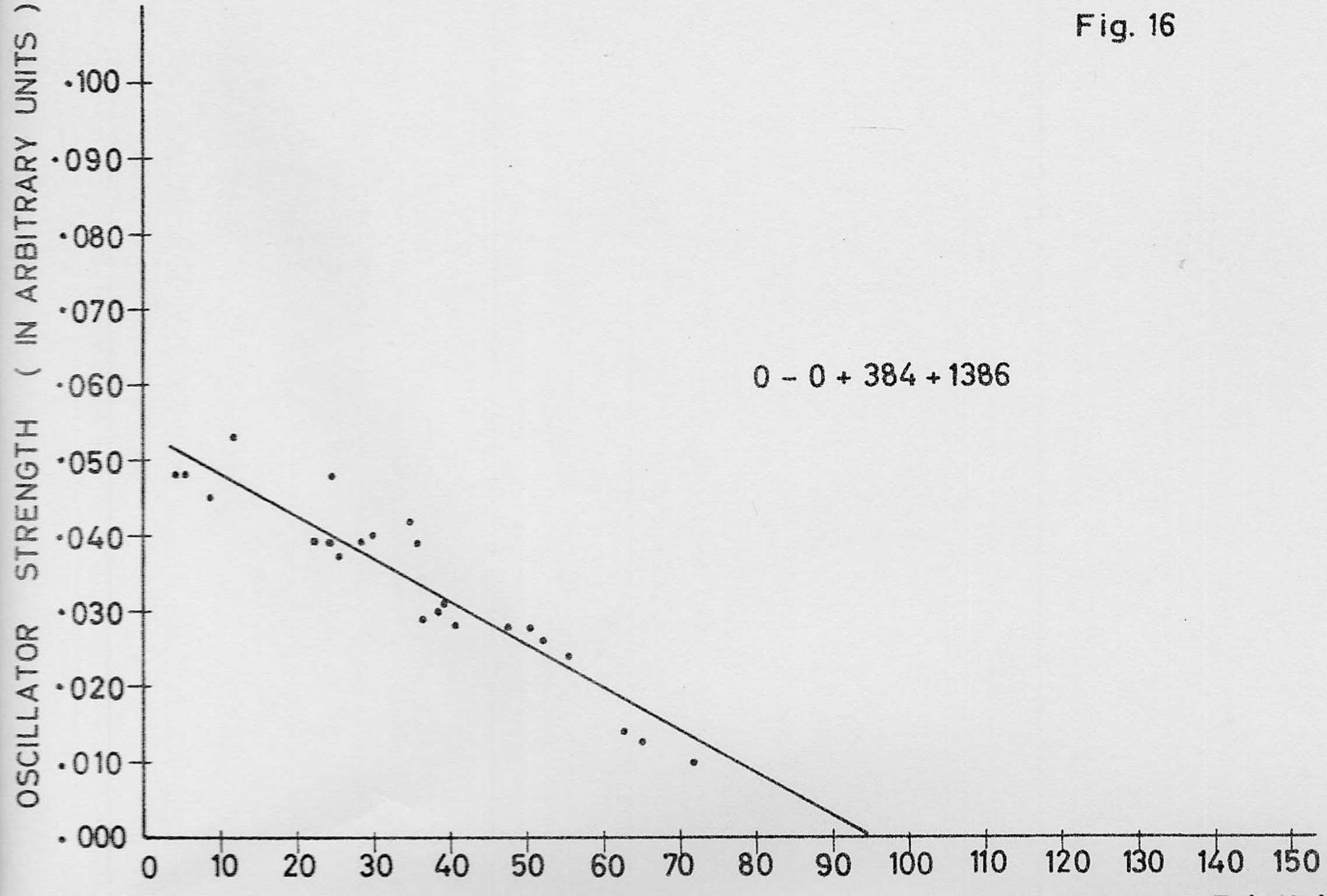
OSCILLATOR STRENGTH (IN ARBITRARY UNITS)
·100
·090
·080
·070
·060
·050
·040
·030
·020
·010
·000
0 10 20 30 40 50 60 70 80 90 100 110 120 130 140 150
0 - 0 + 384 + 1386

Fig. 16

Fig. 17.--Area between 16,510 cm^{-1} and 16,540 cm^{-1} plotted versus temperature.

Fig. 17

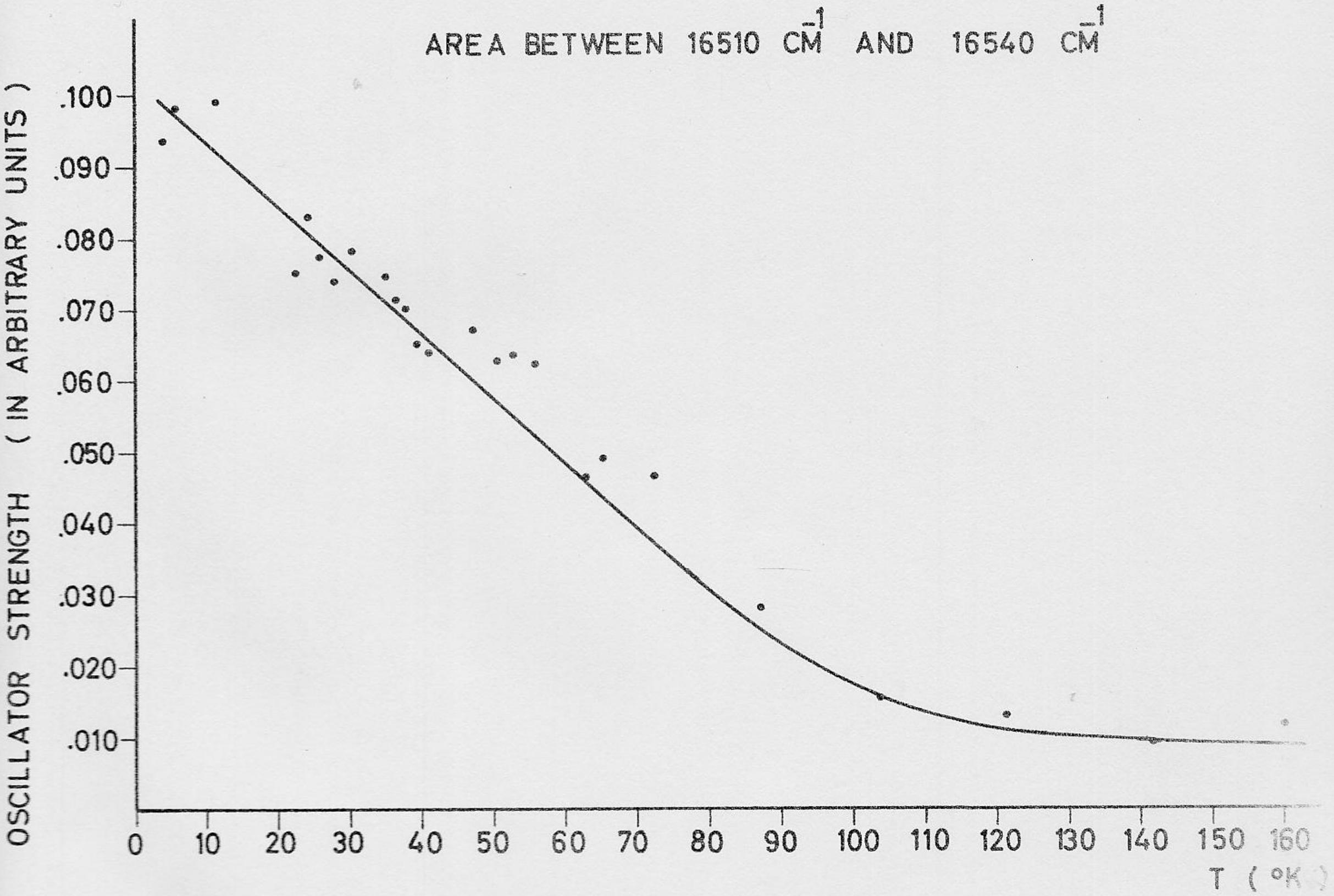
AREA BETWEEN 16510 CM^{-1} AND 16540 CM^{-1}
OSCILLATOR STRENGTH (IN ARBITRARY UNITS)
.100
.090
.080
.070
.060
.050
.040
.030
.020
.010
0
10
20
30
40
50
60
70
80
90
100
110
120
130
140
150
160
T (°K)

Fig. 18.--Oscillator strength (in Arbitrary Units) of the (0-0 + 1191 + 1386) + (0-0 + 2 x 664 + 1386) bands plotted versus temperature.

Fig. 18

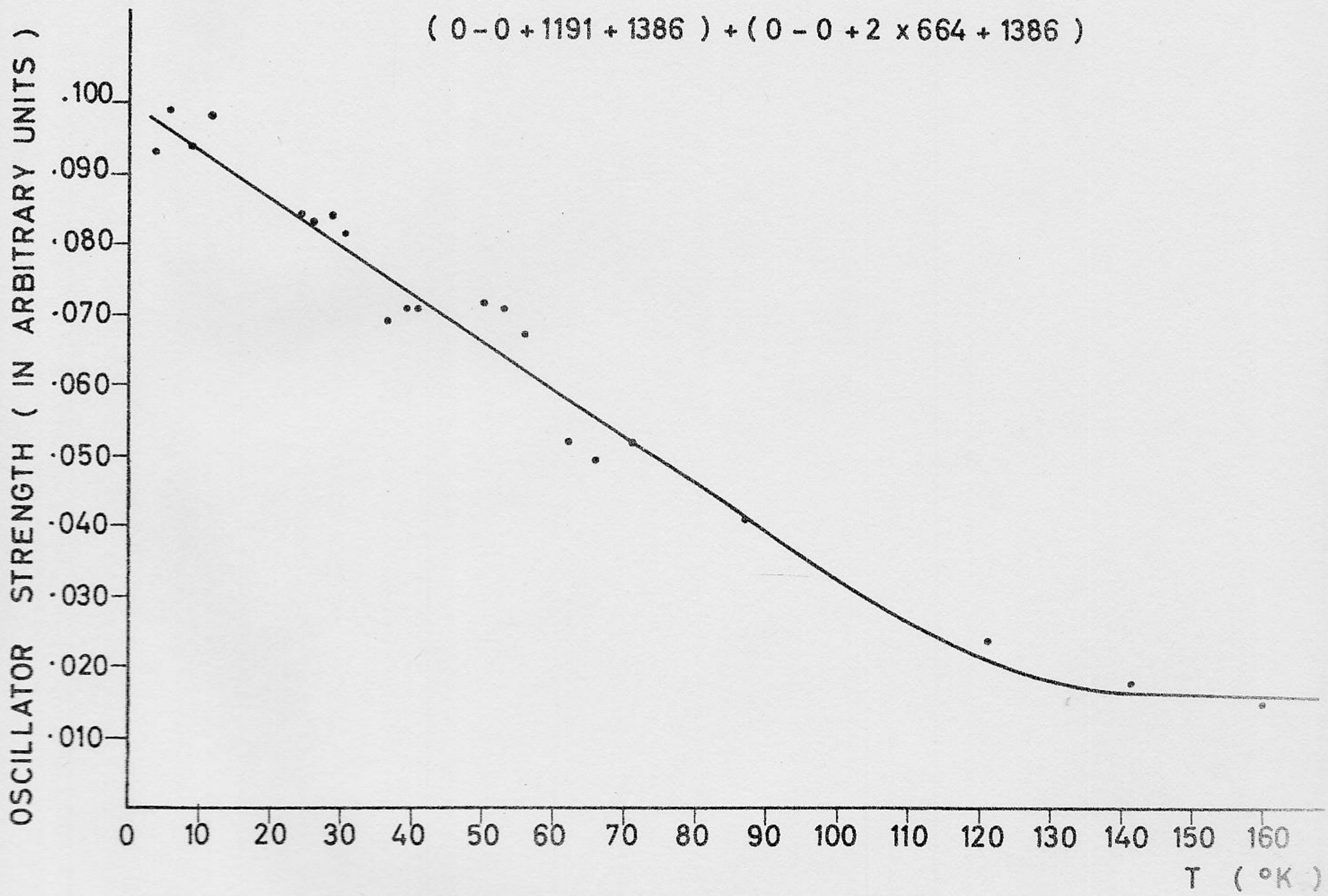
(0 - 0 + 1191 + 1386) + (0 - 0 + 2 x 664 + 1386)
OSCILLATOR STRENGTH (IN ARBITRARY UNITS)
·100
·090
·080
·070
·060
·050
·040
·030
·020
·010
0
10
20
30
40
50
60
70
80
90
100
110
120
130
140
150
160
T (°K)

Fig. 19.--Plot of half-widths versus temperature

Fig. 19

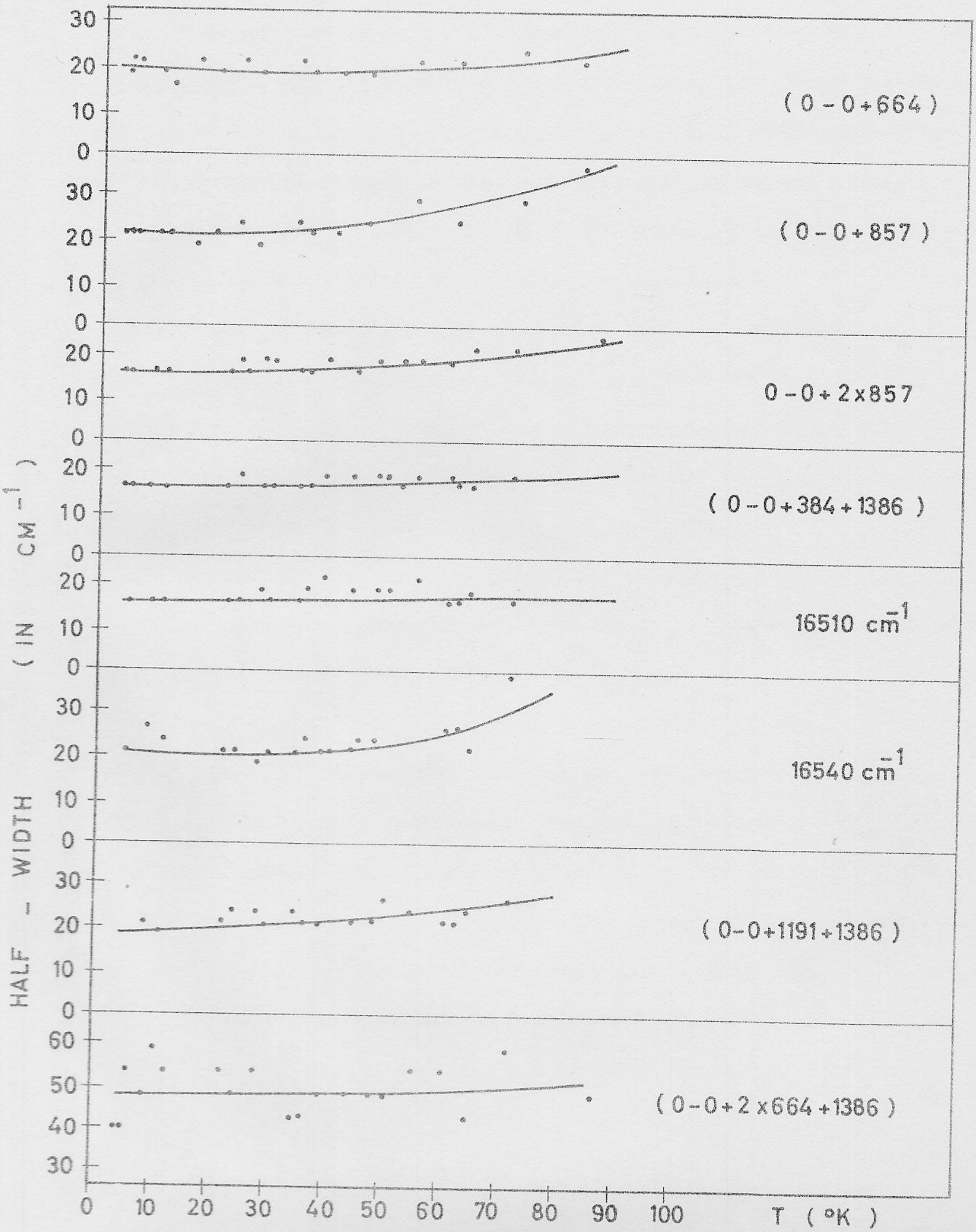
HALF - WIDTH (IN CM^{-1})
30
20
10
0
(0 - 0 + 664)
(0 - 0 + 857)
0 - 0 + 2x857
(0 - 0 + 384 + 1386)
16510 cm^{-1}
16540 cm^{-1}
(0-0+1191+1386)
(0 - 0 + 2 x 664 + 1386)
0 10 20 30 40 50 60 70 80 90 100
T (°K)

V. INTERPRETATION OF RESULTS AND DISCUSSION

The small value (1.7×10^{-2} Pariser[24]; 9×10^{-3} Mann et al[11]) of the oscillator strength is due to a large change in the charge distribution upon electronic excitation. It is thus expected that phonons may induce sufficiently large changes in the polarization of an azulene molecule to alter the charge distribution in either the ground and or the excited state. The results seem to confirm our qualitative expectations.

Figure 20 shows the same absorption bands at three different temperatures. It is clear from this and similar data that the observed decrease in the oscillator strength is not due to a broadening of the lines. The half-width of the single lines and of the envelopes (when two or more lines are included) does not change between 4.2° and $100^{\circ}K$.

Around $50^{\circ}K$ the oscillator strength is weak so that one has to use samples of higher concentration or larger dimensions, and the neighbouring lines may then become unresolved.

The 0-0, 0-0 + 36 and 0-0 + 51 lines exhibit a constant intensity from 4.2° to $55^{\circ}K$. Above $55^{\circ}K$, a higher azulene concentration was used. As a result these lines overlapped. However, the combined area of the three lines shows no significant decrease in intensity up to $300^{\circ}K$. The 20% change seen in Figure 11 for these lines is not significantly greater than the 10 - 15% scatter in the measured areas at high temperatures.

These results show that azulene is not behaving like an oriented gas molecule . The naphthalene phonon field is strongly coupled to the azulene vibronic transitions.

Fig. 20.--Variation of line-shape with temperature

Fig. 20

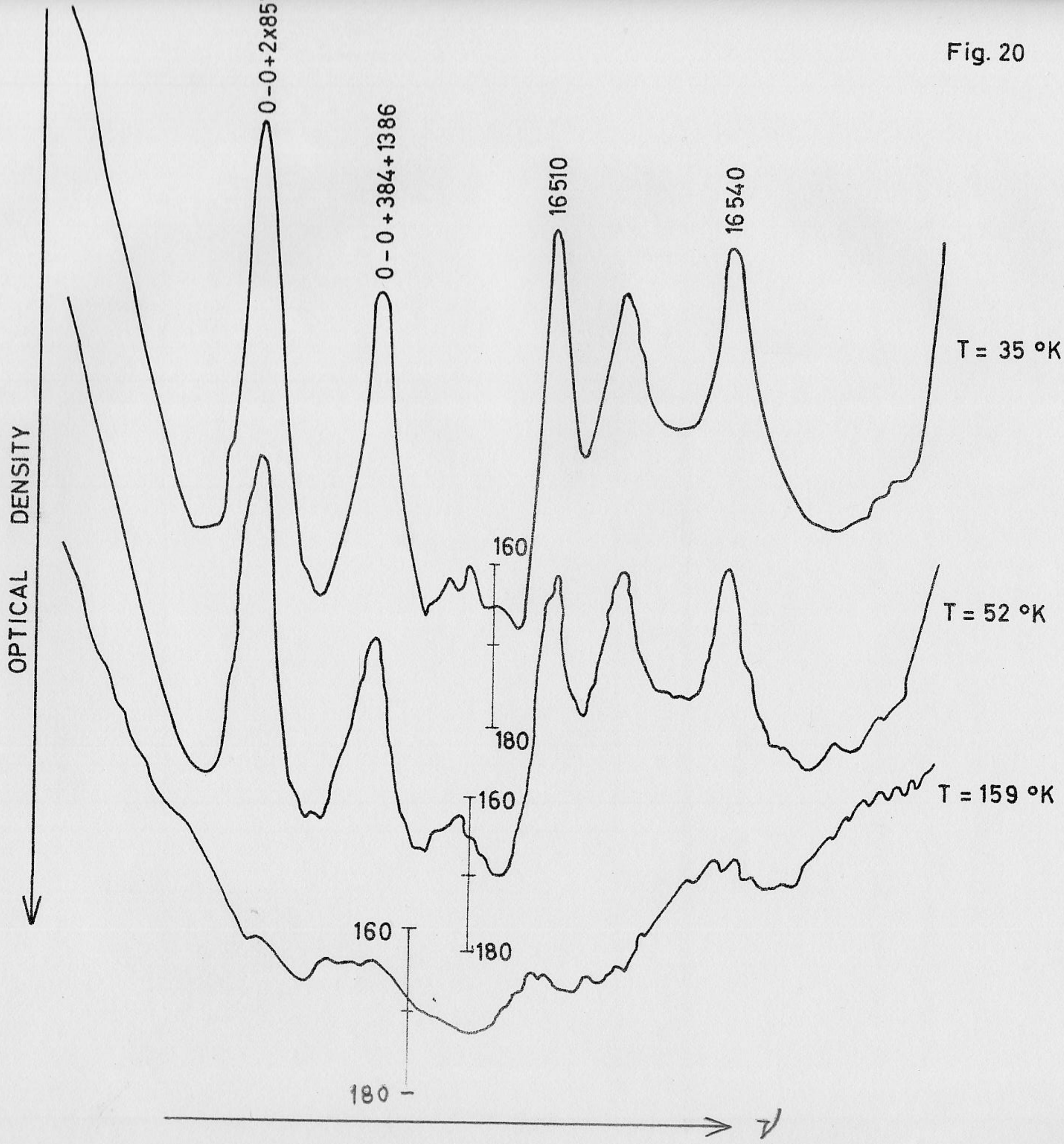
OPTICAL DENSITY
0-0+2x85
0-0+384+1386
16510
16540
T = 35 °K
160
180
T = 52 °K
160
180
T = 159 °K
160
180
ν

At relatively low temperatures where $\frac{f_o - f}{f_o} \leq 0.5$ it appears that the oscillator strength f(T) follows the relation:

$$f = f_o [1 - \alpha \rho(T)] \qquad (6)$$

where $f_o = f(4.2^oK)$, $\rho(T)$ is the phonon occupation probability per unit cell, and α is the coupling constant. For the small azulene concentrations used here, one may assume that there is at most one azulene molecule per unit cell.

TABLE 4

LIST OF THE PHONONS ACTIVE IN THE DIFFERENT BANDS

Vibronic Bands (cm^{-1})	Best Fit Phonon (cm^{-1})	$\alpha \pm .1$ (one branch)
0-0	none	0
0-0 + 664	54	0.9
0-0 + 857	46	0.9
0-0 + 2 x 857	46	0.9
0-0 + 384 + 1386	15	0.2
16,510 - 16,540	15	0.2
0-0 + 1191 + 1386 + 0-0 + 2 x 664 + 1386	15	0.2

Beyond 60^oK, the above relation is not obeyed. Some lattice perturbations must now act to enhance slightly the transition probability to about 5% at 200^oK of its 4.2^oK intensity.

The vibronic transitions 0-0 + 664 are of an intensity slightly greater than that of the 0-0 line. Their integrated intensity seems to be due to coupling with a phonon of wave number 54 cm^{-1}.

Both the 0-0 + 857 and 0-0 + 2 x 857 seem to be affected by a 46 cm^{-1} phonon, whereas the 0-0 + 384 + 1386, 16,510 cm^{-1} - 16,540 cm^{-1} and the 0-0 + 1191 + 1386 bands show a decrease probably due to a 15 cm^{-1} phonon.

The values of α fall into three categories:

(a) $\alpha = 0$ implies that the 0-0 transition is not coupled to the phonons.

(b) $\alpha = 1$ implies that when the phonon occupation number is 1, the transition probability is reduced to zero. In other words, one phonon alters the charge distribution sufficiently to reduce the transition probability to zero. The experimental value of 0.9 ± 0.1 indicates then a strong coupling between the 0-0 + 664, 0-0 + 857 and 0-0 + 2 x 857 vibronic transitions with 54 cm^{-1} and 46 cm^{-1} phonons.

(c) $\alpha \approx 0.2$ implies an intermediate coupling. The vibronic transitions involving the 15 cm^{-1} phonons appear to be weakly coupled.

If we now inquire into the origin of these phonons we meet a number of anomalous results.

The phonons observed by Sidman and McClure have the value 21, 36, 51 cm^{-1} in absorption at 14,652 cm^{-1} and 15, 39, 59 cm^{-1} in the 28,050 cm^{-1} emission system. Rousset[26] studied the Raman spectra of naphthalene and reports that the six naphthalene optical branches have the values: 109, 127, 76, 74, 54 and 46 cm^{-1} for K = 0 at room temperature. Ichishima[27] as quoted by Cruickshank[28] gives the following relations for the temperature dependence of these frequencies between +25°C and -190°C:

$$\nu_4 = 125 - 0.0634T \text{ cm}^{-1} \qquad (106)$$

$$\nu_5 = 145 - 0.0633T \text{ cm}^{-1} \qquad (126)$$

$$\nu_3 = 91 - 0.0593T \text{ cm}^{-1} \qquad (74)$$

$$\nu_1 = 60 - 0.0433T \text{ cm}^{-1} \qquad (47)$$

$$\nu_2 = 75 - 0.0800T \text{ cm}^{-1} \qquad (52)$$

Hence there is a wide divergence between the "observed" optical phonons in emission and absorption on the one hand and the Raman results on the other. It is known from the specific heat studies of crystalline naphthalene that the Raman results are correct for the ground state lattice. It is possible that these rather discrete phonon values are due in one way way or another to the acoustic branches. In the absence of detailed information on the acoustic branches, one is unable to clarify this point. Similar anomalous "optical" phonon frequencies have been reported for a

large variety of molecular crystals by a number of independent workers. The elucidation of this problem may shed considerable light on exciton and electron-lattice interaction processes.

REFERENCES

1. Elsevier's Encyclopedia of Organic Chemistry, eds. E. Josephy and F. Radt, (New York and Amsterdam: Elsevier Publishing Co. Inc., 1948), series III, (Carboisocyclic condensed compounds), vol. 12A, p. 421.

2. M. BEER and H.C. LONGUET-HIGGINS, J. Chem. Phys. 23, 1390 (1955).

3. G. VISWANATH and M. KASHA, J. Chem. Phys. 24, 574 (1956).

4. E. HEILBRONNER and K. WIELAND, Helv. Chim. Acta 30, 947 (1947).

5. G.R. HUNT and I.G. ROSS, J. Mol. Spect. 3, 604 (1959).

6. G.R. HUNT and I.G. ROSS, Proc. Chem. Soc. 11-12 (1961).

7. A. PRIKHOTKO and A. SKOROBOGATKO, Opt. i Spektroskopiya 18, 396 (1965).

8. H.J. MARIA and A.B. ZAHLAN, J. Chem. Phys. 38, 941 (1963).

9. H.J. MARIA, J. Chem. Phys. 40, 551 (1964).

10. J.W. SIDMAN and D.S. McCLURE, J. Chem. Phys. 24, 757 (1956).

11. D.E. MANN, J.R. PLATT and H.B. KLEVENS, J. Chem. Phys. 18, 481 (1949).

12. A.L. SKLAR, J. Chem. Phys. 5, 669 (1937).

13. C.A. COULSON and H.C. LONGUET-HIGGINS, Rev. Sci. Instr. 15, 929 (1947).

14. G.W. WHELAND and D.E. MANN, J. Chem. Phys. 17, 264 (1949).

15. R.D. BROWN, Trans. Faraday Soc. 44, 984 (1948).

16. W. MOFFIT, J. Chem. Phys. 22, 320 (1954).

17. C.C.J. ROOTHAAN, Revs. Modern Phys. 23, 69 (1951).

18. A. JULG, Compt. rend. 239, 1498 (1954).

19. A. JULG, J. Chim. phys. 52, 377 (1955).

20. R. PARISER, J. Chem. Phys. 21, 568 (1953).

21. R. PARISER and R.G. PARR, J. Chem. Phys. 21, 466 (1953).

22. R. PARISER and R.G. PARR, J. Chem. Phys. 21, 767 (1953).

23. J.A. POPLE, Trans. Faraday Soc. 49, 1375 (1953).

24. R. PARISER, J. Chem. Phys. 25, 1112 (1956).

25. J.N. SHERWOOD and S.J. THOMSON, J. Sci. Instrum. 37, 242 (1960).

26. A. ROUSSET, J. Phys. Radium (Ser.8) 9 , 101 (1948).

27. I. ICHISHIMA, J. Chem. Soc. Japan (Pure Chem. Sec.) 71, 607 (1950).

28. D.W.J. CRUICKSHANK, Revs. Modern Phys. 30, 163 (1958).